Comparison of physical- and chemical-activated *Jatropha curcas* husk carbon as an adsorbent for the adsorption of Reactive Red 2 from aqueous solution

Alagarasan Jagadeesh Kumar[a,b], Rajendra Prasad Singh[a,*], Dafang Fu[a,*], Chinnaiya Namasivayam[b]

[a]*Department of Municipal Engineering, Southeast University, Nanjing, Jiangsu 210096, China,*
emails: rajupsc@seu.edu.cn (R.P. Singh), fdf@seu.edu.cn (D. Fu), jaga.jagadeesh1987@gmail.com (A.J. Kumar)
[b]*Department of Environmental Sciences, Bharathiar University, Coimbatore 641046, India, email: cnamasi@gmail.com (C. Namasivayam)*

ABSTRACT

An abundant lignocellulosic agricultural waste of jatropha husk was used to prepare jatropha husk carbon (JHC) and zinc chloride–activated jatropha husk carbon (ZAJHC) as an adsorbent for the removal of Reactive Red 2 (RR2) from water. Batch mode adsorption experiments were carried out and the parameters investigated include agitation time, dye concentration, adsorbent dose, pH and temperature. Adsorption equilibrium data were analyzed using Langmuir, Freundlich, and Dubinin–Radushkevich isotherm models for RR2 concentrations of 20–100 mg L^{-1}. Langmuir adsorption capacity was found to be 12.5 mg g^{-1} for JHC and 100 mg g^{-1} for ZAJHC. The kinetic data are following closely the pseudo-second-order kinetic model. Acidic pH was favorable for the adsorption of RR2. The pH effect and desorption studies suggest that the ion-exchange mechanism might be the major mode of the adsorption process. Significance of this study provides the ZAJHC sample that shows excellent adsorbent toward the removal of RR2 from wastewater.

Keywords: Activated carbon; Adsorption kinetics; Isotherms; jatropha husk; Reactive Red 2

1. Introduction

Textile industry wastewaters are an important source of environmental contamination. The high level of production and application of organic dyes generate colored wastewaters causing serious environmental problems because of their toxicity [1]. Particularly, the textile, mining and metallurgical industries consume enormous volumes of water, and their effluents severely impact the environment because of the toxic nature of their residues [2]. During the last 35 years, China and other developed countries had a major producer of dyes and pigments to cater to the needs of not only the textile industries but also of other industries such as paper, rubber, plastics, paints, printing inks, art and craft, leather, food, drug and cosmetics. Mostly, the reactive dyes are the common dyes used for several applications such as bright colors, excellent color fastness and ease of application [3]. Though not particularly toxic, dyes have an adverse aesthetic effect because they are visible pollutants [4]. The presence of color will reduce aquatic diversity by blocking the passage of light through the water. Therefore, the removal of dyes from strongly colored reactive dye wastewater or effluent becomes environmentally important [5]. It is estimated that approximately 50% of reactive dyes may be lost in the effluent after the dyeing process [6]. There are many techniques for removing dyes from wastewater, such as adsorption, coagulation, filtration, oxidation, sedimentation, precipitation and reverse osmosis. A wide range of technologies have been adopted to remove these dyes from wastewaters.

Adsorption has been found to be an efficient and cost-effective to remove dyes from water [7], various adsorbents

* Corresponding author.

such as activated carbon (AC) [8], sepiolite [9], vermiculite [10] and carbon nanotube [11] were used to remove dyes from aqueous solution. AC is one of the most commonly used adsorbents for removal of dyes from water due to its high specific surface area (SSA) and large adsorption capacity [12]. The widespread cultivation of *Jatropha curcas* is initiated globally. According to the Planning Commission of India, the estimated potential area of *J. curcas* plantations is 17.4 million hectares and the projected jatropha husk (JH) production is 350 million tons [13].

As JH is rich in lignin, it has the potential to be a good precursor for the production of AC, which forms the basis of this work [14]. The waste biomass has been utilized by many researchers for removal of Reactive Red 2 (RR2) using ACs prepared by different activators such as coir pith H_2SO_4 [15], rice husk by H_2SO_4 [16], H_3PO_4 and $ZnCl_2$-activated buriti shells [17]. Since $ZnCl_2$ is a dehydrating agent, formation of tar on activation of the precursor can be avoided [18] as carbonaceous precursors for the removal of dyes from wastewater. The objective of the present study was to evaluate the comparison of jatropha husk carbon (JHC) and zinc chloride–activated jatropha husk carbon (ZAJHC) for the removal of RR2 from aqueous solution. Adsorption isotherms were studied at different RR2 concentrations. Desorption was performed under controlled conditions to check the reversibility in the adsorption process and desorption yield from a loaded adsorbent was measured at different pH values.

2. Experimental

2.1. Materials

jatropha husk (JH) was collected from Tamil Nadu Agricultural University, Coimbatore, India. The dry raw JH was washed with tap water and then washed with double-distilled water to remove earthy impurities. Then it was dried in a hot air oven at 105°C ± 5°C for 8 h. All the chemicals used are AR grade and were purchased from Loba-Chem and Merck (Mumbai, India).

2.2. Synthesis of JHC by physical method

The JH was collected and further it was washed, dried and crushed in a steel container with a tight lid. This container was placed in another concentric steel container with another lid. The linear space was filled with sand that was consolidated layer by layer up to the brim of the outer container. This arrangement achieved a near-total absence of exposure of the carbonizing material, allowing only a limited presence of oxygen trapped in the voids of the JH. This setup was placed in a muffle furnace for 1 h at 800°C ± 5°C. After down to room temperature, the carbon was collected and washed with distilled water to remove impurities like tars. This material was subsequently oven-dried at 105°C ± 5°C for 8 h and sieved to 250–500 mm (60–35 mesh American Standard Test Sieve Series (ASTM)) size and designated as JHC.

2.3. Synthesis of ZAJHC by chemical method

The washed, dried and crushed JH (450 g) was mixed with 2.0 L hot water containing 450 g of $ZnCl_2$ for 1 h. The remaining solution was drained off and $ZnCl_2$-soaked JH was dried using oven at 60°C ± 5°C for 12 h. The material was filled in a steel container (19 cm × 9 cm × 9 cm) with a tight lid. This container was placed in another concentric steel container (29 cm × 12 cm × 12 cm) with another lid. The linear space was filled with sand, which was a consolidated layer by layer up to the brim of the outer container. This arrangement achieved a near-total absence of exposure of the carbonizing material to air, allowing only a limited presence of oxygen trapped in the voids of the ZAJHC. This setup was placed in a muffle furnace at 1 h at 800°C ± 5°C. After down to room temperature, the carbon was taken out and the excess zinc chloride was leached out by immersing it in hot 1.0 M HCl solution for 24 h and kept in an air oven at 80°C ± 5°C. It was then repeatedly washed with hot water until the chloride had disappeared from the wash water (tested by the silver nitrate method). This material was subsequently oven-dried at 105°C ± 5°C for 8 h and sieved to 250–500 μm size (60–35 mesh ASTM) and designated as ZAJHC and stored in airtight plastic container. All the chemicals used are of analytical reagent grade from Loba Chemie Ltd. and Merck Ltd. (Mumbai, India).

2.4. Characterization

The surface characteristics of JHC and ZAJHC such as pH, specific gravity, bulk density (g⁻¹ mL), porosity, ion-exchange capacity, solubility in water and acid, availability of iodine number, pH_{zpc}, S_{BET} surface area, and pore distribution are shown in Table 1. The isoelectric point (IEP) or zeta potential zero point charge (pH_{ZPC}) is an essential factor that constructs the adsorption capacity of the AC. AC is usually considered as amphoteric solid due to the existence of variety of surface functional groups. The pH_{ZPC} value is the point at which surface functional groups do not contribute to the pH of the solution. IEP is used to qualitatively assess the polarity of the adsorbent surface charge. The pH_{ZPC} of the ZAJHC is 6.80. At pH < IEP, the adsorbent has positive surface charge and can act as anion exchanger. While at pH > IEP, the surface charge of the adsorbent is negative, which benefits for adsorbing cations. Structural studies and surface morphologies of the loaded and unloaded ZAJHC were characterized by different analytical techniques. X-ray diffraction was performed at room temperature using a PAN analytical (X-Pert-Pro) diffractometer with Cu $K\alpha_1$ radiation (λ = 1.5406 Å). Infrared spectrum of the samples was obtained by using a Fourier transform infrared (FTIR) spectrometer (Bruker Tensor 27, Germany). The X-ray photoelectron spectroscopy (XPS) was carried out using a Kratos Axis

Table 1
Characteristics of JHC and ZAJHC

S. no.	Characteristics	JHC	ZAJHC
1	pH_{zpc}	9.7	6.8
2	Specific gravity	0.05	1.03
3	Bulk density (g L⁻¹)	0.29	0.20
4	Porosity (%)	84	81
5	S_{BET} (m² g⁻¹)	424	822
6	Iodine number (mg g⁻¹)	70	91

Ultra-DLD X-ray photoelectron spectroscope (Manchester, UK). The morphology and elemental analysis of the loaded and unloaded ZAJHC were examined using scanning electron microscope (SEM-JSM, 840A, JEOL, Japan). The carbon samples were filtered using a suction pump on qualitative filter paper and stored in a vacuum desiccator, which was later used for instrumental analysis.

2.5. Preparation of RR2 solutions

A stock solution was prepared by dissolving an appropriate quantity of RR2 (1,000 mg L^{-1}) in distilled water. A calibration plot was prepared by measuring the absorbance at 508 nm using UV–visible spectrometer (SPECORD 200, Analytic Jena, Germany). The working solutions were prepared (20–100 mg L^{-1}) by diluting the stock solution with distilled water to give the appropriate concentration of the working solutions.

2.6. Batch mode adsorption study

Adsorption experiments were carried out by agitating 50 mg of ZAJHC with 50 mL of dye solution of desired concentration and pH at 200 rpm, 35°C in a thermostated rotary shaker (Orbitek, Chennai, India). RR2 concentration was estimated spectrophotometrically by monitoring the absorbance at 508 nm using UV–Vis spectrophotometer (Specord 200, Analytic Jena, Germany). The pH was measured using pH meter (Elico, model LI-127, Hyderabad, India). The dye solution was separated from the adsorbent by centrifugation at 2,500 rpm for 30 min and its absorbance was measured. Effect of adsorbent dosage was studied with different adsorbent doses (25–200 mg) and 50 mL of dye solutions and agitated for equilibrium time. Langmuir, Freundlich and Dubinin–Radushkevich (D–R) isotherms were employed to study the equilibrium adsorption. Effect of pH was studied by adjusting the pH of dye solutions using dilute HCl and NaOH solutions and the solutions were agitated with 50 mg/50 mL. JHC and ZAJHC desorption studies of the adsorbent that was used for the adsorption of 20 and 40 mg L^{-1} of dye solution was separated from the solution by centrifugation. The dye-loaded adsorbent was filtered using Whatman filter paper and washed gently with water to remove any unabsorbed dye. Several such samples were prepared. Then the spent adsorbent was agitated for 120 min with 50 mL of distilled water and adjusted to different pH values. The desorbed dye was estimated as before. Effect of temperature on removal was examined using aliquots of 50 mL RR2 solution of 60 mg L^{-1} with 25 mg of JHC and ZAJHC was carried out at 35°C, 40°C, 50°C and 60°C.

3. Results and discussion

3.1. Structural and morphological analysis

3.1.1. X-ray analysis

X-ray powder diffraction pattern was used to analyze the crystallinity and phases of the as-prepared JHC and ZAJHC as RR2 adsorbed JHC and ZAJHC. Fig. 1(a) shows broad peaks at 23.5° and 43°, which correspond to the (002) and (100) planes, respectively. Thus, the results confirm that the

ZAJHC was amorphous. The XRD pattern of RR2-adsorbed ZAJHC shows that the intensity of (002) and (100) planes are slightly suppressed Figs. 1(a) and (b) [19]. The decreased intensity of the planes may be due to the adsorbed RR2 on the surface and pores of ZAJHC.

3.1.2. FTIR analysis

The FTIR spectra of the JHC and ZAJHC and RR2 adsorbed JHC and ZAJHC are shown in Figs. 1(c) and (d). The FTIR spectrum of the AC shows weak and broad peaks in the region of 500–4,000 cm^{-1}. Many bands disappeared, indicating the vaporization of organic matters present on precursor (JHC). This confirms that due to complete decomposition/volatilaztion of precursor most of the surface functional groups present on JHC disappeared or got washed out, though some peaks are observed in FTIR spectrum of ZAJHC. The wide band at 3,425 cm^{-1} is due to the O–H vibrations of hydroxyl groups. The development of ZAJHC intense band occurred at about 2,923 cm^{-1} for the removal of RR2 precursor and was attributed to the C–H
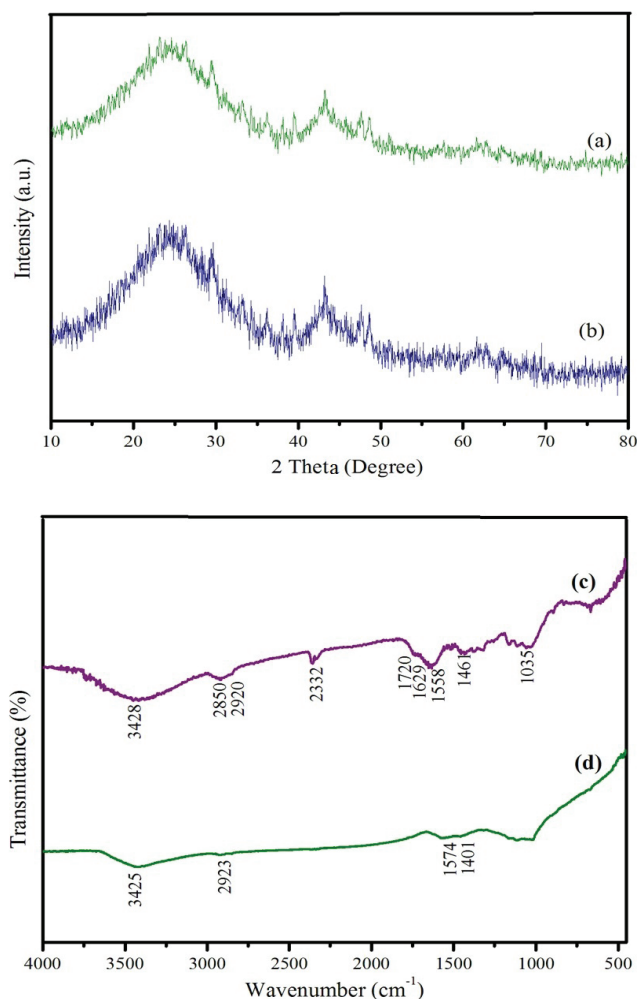
Fig. 1. Before adsorption of X-ray patterns JHC (a), after adsorption of X-ray patterns ZAJHC (b), before adsorption of FTIR JHC (c), after adsorption of FTIR ZAJHC (d).

stretching vibration. It disappeared due to the elimination of hydrogen elements to a large extent when using AC. In addition, ZAJHC observed that the sharp bands at about 1,035 cm^{-1} for the sludge precursor shifted toward higher wave number for ACs indicating some changes in the C–O–C group in carboxylic and alcoholic groups [20]. The RR2-loaded ZAJHC shows peak at 1,574 cm^{-1} which was shifted into 1,570 cm^{-1} and can be attributed to N–H vibration coupled with C–N stretching mode, indicating the saturation of the material with the RR2 [21].

3.1.3. XPS analysis

XPS was employed to analyze the structure of carbon and AC and also to confirm the results obtained by the Raman spectroscopy. The amounts of surface functional groups (acidic and basic) of JHC and ZAJHC were as 5.67 (36.79%), 9.74 (63.21%), 1.46 (86.9%) and 0.22 (13.1%) meq g^{-1}, respectively. The total functional of groups of JHC and ZAJHC such as 15.41 (100%) and 1.68 (100%) meq g^{-1}, respectively. The XPS spectra of JHC and ZAJHC show strong signals from carbon and oxygen elements as shown in Fig. 2, JHC exhibits two prominent peaks attributed at 285.3 and 533.8 eV. The C 1s core level peak positions of the carbon atoms were at 285.3 eV. Fig. 2 shows the peak position for oxygen which was centered on 533.8 eV. The XPS spectrum of ZAJHC exhibits two peaks attributed at 285.5 eV and 533.5 eV corresponding to C 1s and O 1s, respectively [21].

3.1.4. Morphological analysis

In the present study, the SEM images of the external surface of thermally activated jatropha husk carbon (JHC and ZAJHC) was full of cavities and was very irregular growth-like structure (Fig. 3). The results showed that the change in fractal dimension was insignificant and the complete development of pores on the surface of ZAJHC was due to the activation of ZnCl$_2$ [22]. Morphology of the JHC and ZAJHC and RR2 loaded were observed through SEM micrographs and Fig. 3(b) shows tremendous, perfect and constructed pore structures on the surface. The carbon is compressed and the lanky structure is due to the formation of more interspaces between the monolayers of the carbon by activation of ZnCl$_2$. Higher volume of pores developed from the ZnCl$_2$ activation acts as a route for the contaminants to enter into the micropores. Basically, the high SSA and pore structure are the basic parameters for an effective adsorbent. When the porosity of the JHC and ZAJHC increases, the SSA also increases. After adsorption, the surface turned to irregular structure. It showed that the dye was strongly adsorbed on the surface of the JHC and ZAJHC as shown in Figs. 3(a)–(d).

3.2. Adsorption of RR2 on ZAJHC

3.2.1. Effect of pH

The effect of initial pH solution removal of RR2 (20–100 mg L^{-1}) on JHC and ZAJHC. The pH dependence of dye adsorption onto JHC and ZAJHC adsorbents could
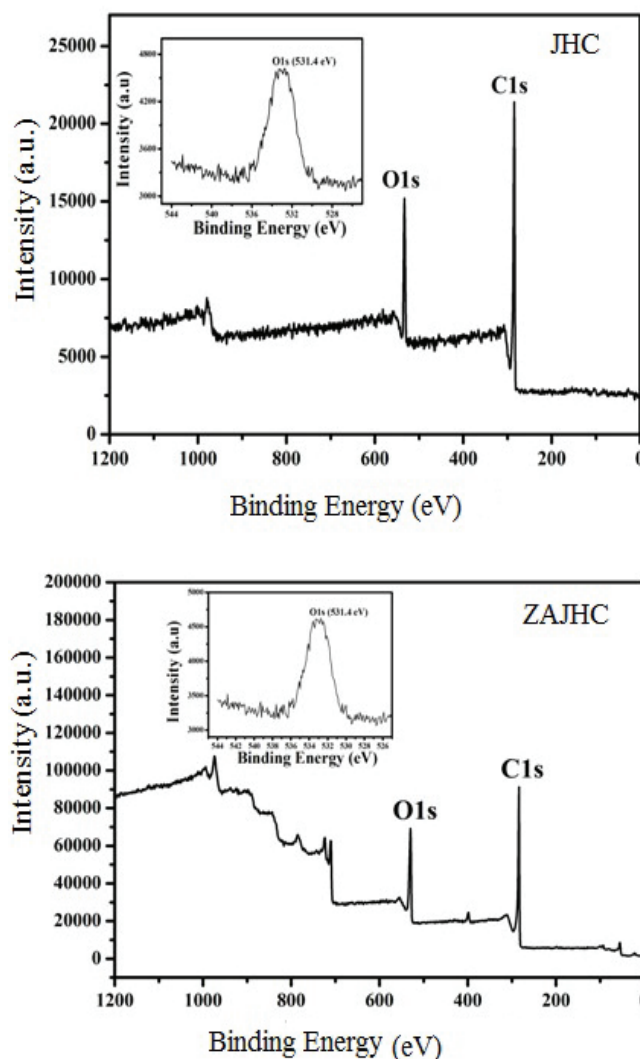
Fig. 2. XPS spectra of JHC and ZAJHC.

be well explained in terms of their pH$_{ZPC}$. When pH < pH$_{ZPC}$, the net surface charge on solid surface of JHC and ZAJHC adsorbents is positive due to adsorption of excess H$^+$, which favors adsorption of dye anion due to Coulombic attraction. At pH > pH$_{ZPC}$, the net surface charge is negative due to desorption of H$^+$ and adsorption must compete with Coulombic repulsion. The consistent RR2 removal in the pH range 2–10, JHC 15%–2% and ZAJHC 98%–23% could be due to the combined effect of both chemical and electrostatic interactions between adsorbent surfaces and SO$_3^-$ in dye anions. The observed reduction in dye adsorption above pH 10.0 may suggest that the strong negative surface charge developed may cause repulsion for the available adsorption sites. Another factor is that in alkaline medium, lower adsorption capacity may be due to the competition of OH$^-$ ions with dye anions [23]. The decrease in dye adsorption is particularly sharp above pH 10.0, as the surface charge becomes more negative. Hence, dye anions would have to overcome electrostatic forces as there would be a higher density of negative charge very close to the surface, hence greater electrostatic repulsion.
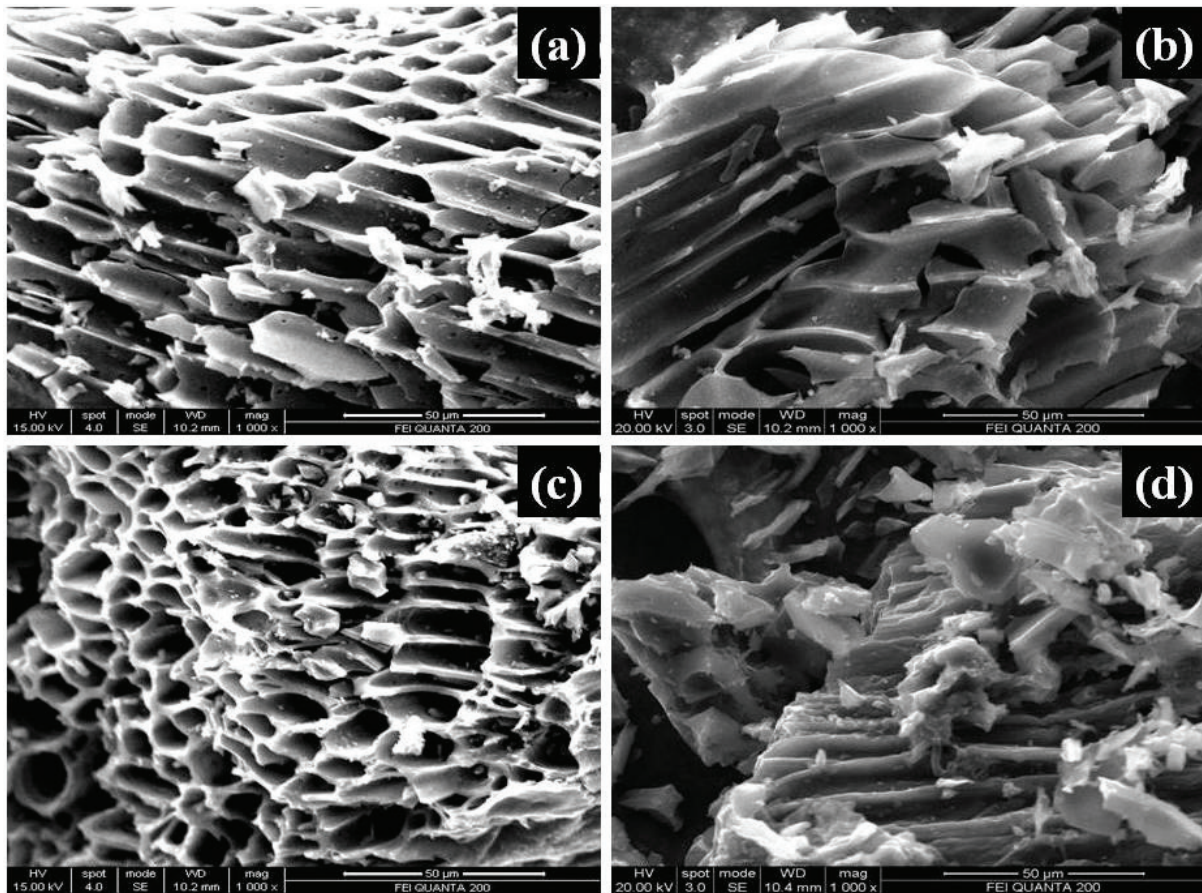
Fig. 3. SEM images of (a) raw JHC, (b) JHC with adsorbed RR2, (c) raw ZAJHC, and (d) ZAJHC with adsorbed RR2.

3.2.2. Desorption studies

Disposal of the spent adsorbent directly or indirectly pollutes the environment. If regeneration of adsorbate from the spent adsorbent is possible, then it would not only protect the environment but also help to recycle the adsorbate and adsorbent for further use and hence contribute to the economy of treatments. Desorption studies also aid to evaluate the adsorption mechanism. Desorption studies as a function of pH were conducted to analyze the possibility of reuse of the adsorbent for further adsorption and to make the process more economical. The desorption process was conducted with two different dye concentrations of 20 and 40 mg L^{-1}. As the pH increases, the desorption percentage gradually increases as shown in Figs. 4(c) and (d). The reversibility of adsorbed dyes is in agreement with the pH dependent results obtained. Desorption of dye at higher pH indicates that the adsorption of RR2 by JHC and ZAJHC was spontaneous and it was followed by an ion-exchange mechanism.

3.2.3. Effect of agitation time

A sequence of contact time JHC and ZAJHC experiments for adsorption of RR2 were carried out at different initial concentrations (20–100 mg L^{-1}) at 35°C shown in Figs. 5(a) and (b). RR2 amount adsorbed increased from 2.0 to 5.92 mg g^{-1} with an increase in initial concentration from 20 to 100 mg L^{-1}

of JHC. In the case of RR2, the amount adsorbed increased from 14.84 to 58.03 mg g^{-1} with an increase in initial concentration from 20 to 100 mg L^{-1} at initial pH solution 6.0, respectively. The JHC equilibrium time was found to be 80 min for 20 mg L^{-1}, 120 min for other concentrations. In the case of ZAJHC equilibrium time was found to be 100 min for all the concentrations. The percent of removal decreased with increasing initial concentration of dye, but the actual amount of dyes adsorbed per unit mass of carbon increased with increase in the concentration of dyes. It means that the adsorption is highly dependent on initial concentration of dyes. At lower concentration, the ratio of the initial number of dye molecules to the available surface area is low. Subsequently, the fractional adsorption becomes independent of initial concentration. However, at the high concentration of dye, the available sites of adsorption become fewer and hence the percent removal of dyes is dependent upon initial concentration.

3.2.4. Effect of adsorbent dose

The increase in adsorbent dose increased the percent removal and attained a plateau after a particular adsorbent dose. A larger mass of adsorbent could adsorb larger amount of adsorbate due to the availability of more surface area of the adsorbent. Removal of RR2 by JHC and ZAJHC at different adsorbent doses from 25 to 200 mg/50 mL and different initial concentrations of RR2 from 20 to 100 mg L^{-1} was studied. It was
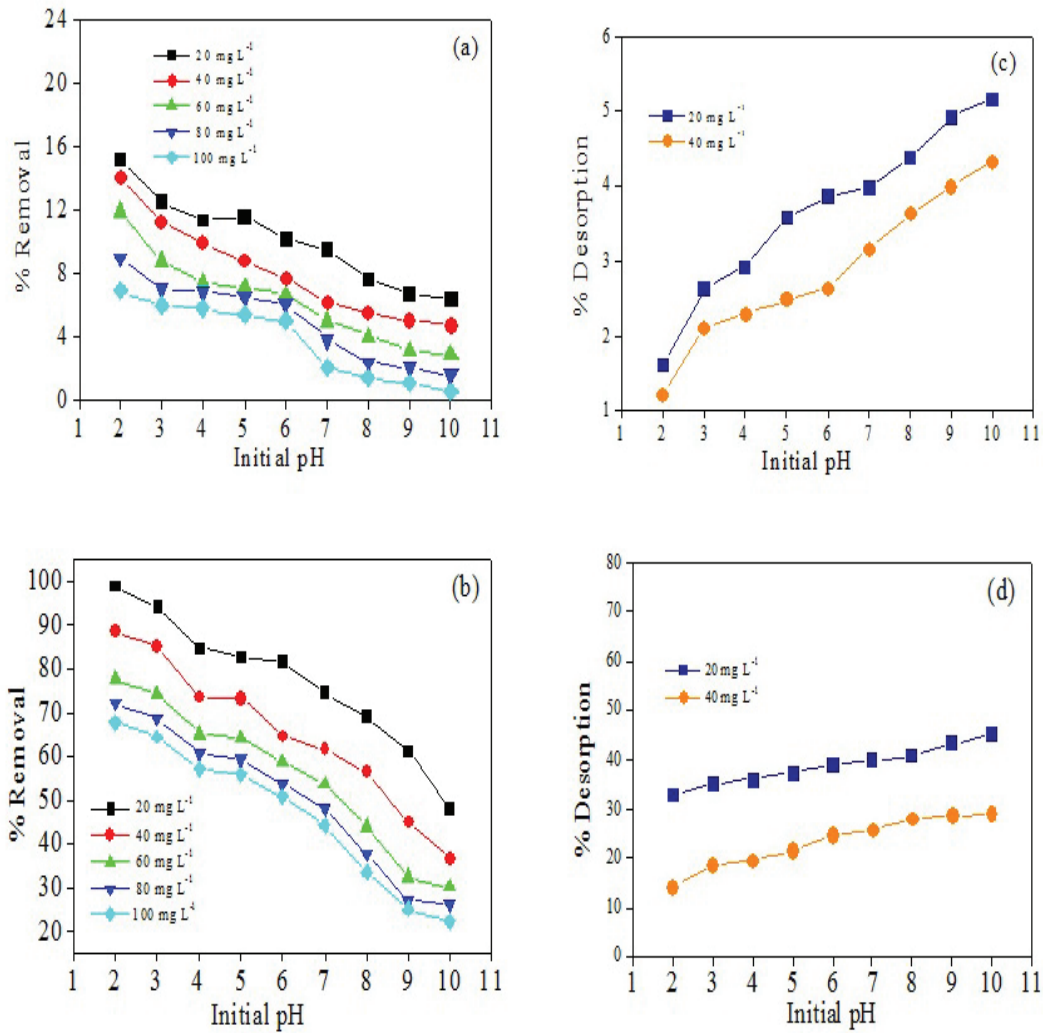
Fig. 4. Effect of pH on (a,b) JHC and ZAJHC adsorption of RR2 and (c,d) JHC and ZAJHC desorption of RR2.

found that increase in adsorbent dose increased the removal of RR2 and quantitative removal occurred at 25, 50, 75, 100, 150 and 200 mg/50 mL for 20, 40, 60, 80 and 100 mg L^{-1} of RR2, respectively. However, for each adsorbate studied, the amount of adsorbate adsorbed (q_e) after equilibrium per unit weight of adsorbent was different for JHC and ZAJHC. In the case of ZAJHC percent removal increased to 100% with increase in adsorbent dose for all the dyes. In the case of JHC, the percent removal did not reach 100% even though the adsorbent dose was increased. The equilibrium pH (final pH after adsorption) of the adsorbate plays an important role in the adsorption process. As adsorbent dose was increased, the final pH for the adsorption of dyes also generally increased slightly.

3.2.5. Adsorption kinetics

The rate constant of adsorption is determined from the first-order rate expression given by:

$$\log(q_e - q) = \log q_e - \frac{k_1 t}{2.303} \tag{1}$$

where q_e and q are the amounts of RR2 adsorbed (mg g^{-1}) at equilibrium and at time t (min), respectively, and k_1 is the rate constant of adsorption (min^{-1}). Linear plots of $\log(q_e - q)$ vs. t for different concentrations of RR2 were obtained. Table 2 shows the values of k_1, which were calculated from the slopes of the linear plots.

3.2.5.1. Pseudo-second-order kinetic model Second-order kinetic model can be represented as follows:

$$\frac{t}{q} = \frac{1}{k_2 q_e^2} + \frac{1}{q_e} \tag{2}$$

where k_2 is the equilibrium rate constant of pseudo-second-order adsorption (g mg^{-1} min^{-1}). Values of k_2 and q_e were calculated from the plots of t/q vs. t. The computed results obtained from the first- and second-order kinetic models along with experimental q_e values are presented in Table 2. The calculated q_e values of the pseudo-second-order
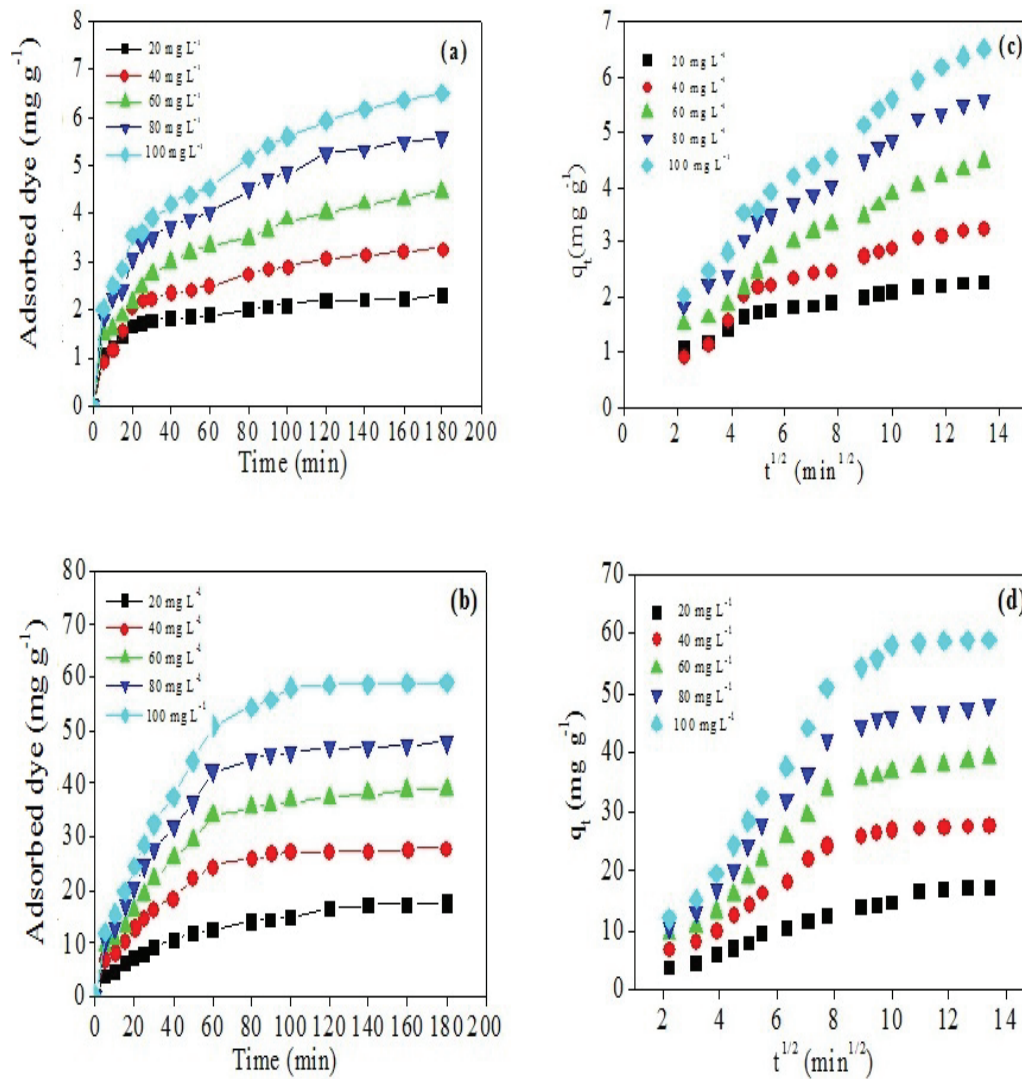
Fig. 5. Effect of agitation time and initial RR2 concentration on (a) JHC and (b) ZAJHC; intraparticle diffusion plots for adsorption of RR2 onto (c) JHC and (d) ZAJHC.

Table 2
Kinetic parameters for the removal of RR2 onto JHC and ZAJHC

Adsorbent	Initial conc. (mg L^{-1})	q_e (exp) (mg g^{-1})	Pseudo-first order			Pseudo-second order		
			k (min^{-1})	q_e (cal) (mg g^{-1})	R^2	K_2 (g mg^{-1} min^{-1})	q_e (cal) (mg g^{-1})	R^2
JHC	20	2.00	0.04	1.04	0.937	0.14	2.09	0.997
	40	3.09	0.02	2.01	0.961	0.07	3.39	0.993
	60	4.02	0.03	3.03	0.958	0.04	4.50	0.99
	80	5.25	0.02	3.63	0.981	0.03	5.71	0.986
	100	5.92	0.02	4.38	0.969	0.03	6.58	0.986
ZAJHC	20	14.84	0.035	16.03	0.978	0.0017	17.86	0.984
	40	27.01	0.044	34.91	0.966	0.0007	28.57	0.998
	60	36.75	0.044	48.75	0.967	0.0004	37.04	0.987
	80	45.87	0.051	70.46	0.941	0.0003	45.45	0.974
	100	57.04	0.039	67.76	0.967	0.0002	55.56	0.981

kinetics are generally closer to the experimental q_e values compared with calculated q_e values from pseudo-second-order kinetics. Therefore, the adsorption process follows pseudo-second-order kinetic model. Similar results were also obtained for the adsorption kinetics of various pollutants onto AC cloth [24–27].

3.2.6. Intraparticle diffusion

An empirically found functional relationship, common to the most adsorption processes, is that the uptake varies with $t^{1/2}$. It is represented as follows:

$$q_t = k_{id} t^{1/2} \tag{3}$$

where q_t is the amount adsorbed (mg g^{-1}) at time, t (min) and k_{id} is the intraparticle diffusion rate constant. Plots of q_t vs. k_{id} have the same general features (Figs. 5(c) and (d)). The initial curved portion is attributed to the bulk diffusion effect, the linear portion to the intraparticle diffusion effect and the plateau to the equilibrium. The linear portions of the plots do not pass through the origin indicating that intraparticle diffusion is not the only rate controlling step for adsorption process. The slopes of the linear portions of the plots of q_t vs. $t^{1/2}$ give the values of k_{id} (Table 3). Values of intercept give an idea about the thickness of boundary layer, that is, larger the intercept, greater is the boundary layer effect [28]. The linear portions are attributed to the instantaneous utilization of the most readily available adsorbing sites on the adsorbent surface.

3.2.7. Adsorption isotherms

Adsorption isotherms are mathematical models, which are used to describe the distribution of the adsorbate species among solid and liquid phases. The adsorption data were investigated by using three types of the most common isotherms: Langmuir, Freundlich and D–R models shown in Figs. 6(a) and (b).

3.2.7.1. Langmuir isotherm Langmuir model suggests a monolayer adsorption with no lateral interaction between the adsorbed molecules. Langmuir equation is expressed as follows [29]:

$$\frac{C_e}{q_e} = \frac{1}{Q_0 b} + \frac{C_e}{Q_0} \tag{4}$$

The constant Q_0 gives the theoretical monolayer adsorption capacity (mg g^{-1}) and b is related to the energy of adsorption (L mg^{-1}). Plot of C_e/q_e vs. C_e gives a straight line with slope $1/Q_0$ and intercept $1/Q_0 b$. JHC and ZAJHC Langmuir constants Q_0 and b were found to be 12.5 mg g^{-1} and 0.01 (L mg^{-1}), 100 mg g^{-1} and 0.03 (L mg^{-1}), respectively. The essential characteristics of the Langmuir isotherm can be expressed by a dimensionless constant called equilibrium parameter R_L. The calculated R_L values were found to be between 0 and 1 that indicate favorable adsorption. The R_L values are shown in Table 4.

3.2.7.2. Freundlich isotherm Freundlich model assumes heterogeneous adsorption due to the diversity of sorption sites or the diverse nature of the adsorbate adsorbed, free or hydrolyzed species.

The Freundlich isotherm model is expressed as follows [30]:

$$\log q_e = \log k_f + \frac{1}{n} \log C_e \tag{5}$$

The Freundlich constants, k_f and n, were calculated from the linear plot of $\log q_e$ vs. $\log C_e$ and are presented in Table 4. Similar results were also obtained for the adsorption isotherm data of various pollutants onto AC cloth [31–33].

3.2.7.3. Dubinin–Radushkevich This adsorption potential is independent of temperature, but it varies depending on the nature of adsorbent and adsorbate. The mean free energy of adsorption gives information about adsorption mechanism as chemical ion exchange. If E value is between 8 and 16 kJ mol^{-1}, the adsorption process follows by ion exchange and if $E < 8$ kJ mol^{-1}, the adsorption process

Table 3

Intraparticle diffusion kinetic parameters of RR2 onto JHC and ZAJHC

	Conc. (mg L^{-1})	q_e(exp)(mg g^{-1})	k_{id} (mg g^{-1}h$^{-1/2}$)	C	R^2
	20	2.00	0.10	1.09	0.897
	40	3.09	0.19	0.93	0.901
Intraparticle	60	4.02	0.27	1.03	0.967
diffusion JHC	80	5.25	0.34	1.40	0.97
	100	5.92	0.40	1.49	0.979
	20	14.84	1.32	1.51	0.972
	40	27.01	2.07	4.37	0.894
Intraparticle	60	36.75	2.95	4.93	0.906
diffusion ZAJHC	80	45.87	3.64	6.40	0.893
	100	57.04	4.70	5.72	0.905
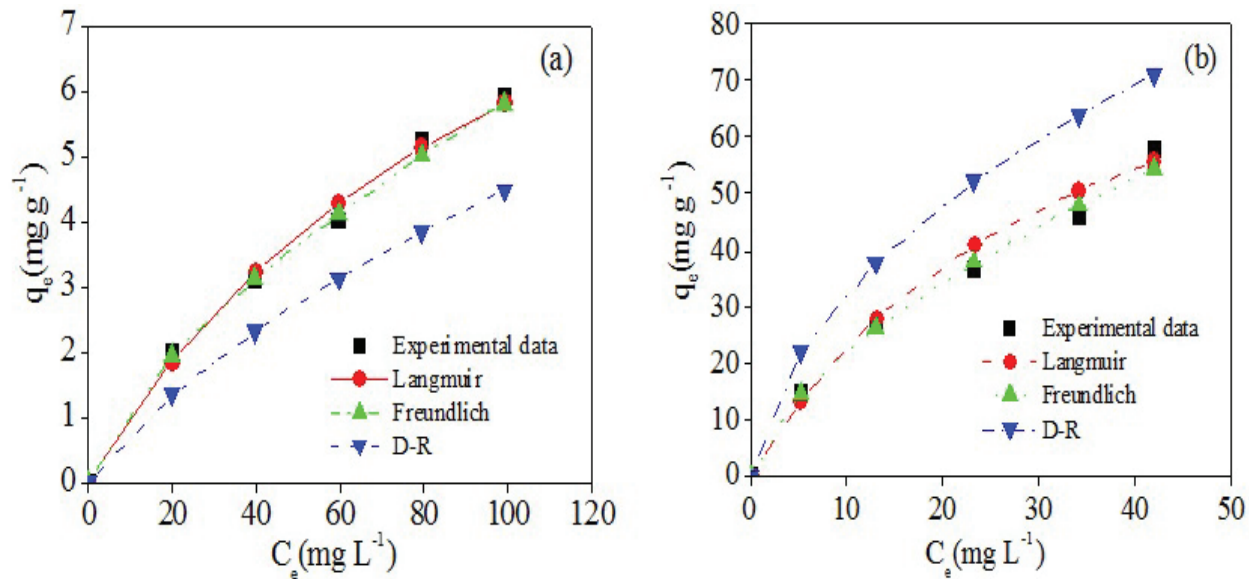
Fig. 6. Comparison of Langmuir, Freundlich and D–R isotherms for adsorption of RR2 onto (a) JHC and (b) ZAJHC.

Table 4
Langmuir, Freundlich and Dubinin–Radushkevich isotherm constants for the adsorption of RR2 onto JHC and ZAJHC

Adsorption system	Conc. mg L^{-1}	Langmuir					Freundlich				D–R			
		Q_0 (mg g^{-1})	b (L mg^{-1})	R^2	R_L	Δq (%)	k_f mg$^{1-1/n}$ L$^{1/n}$/g	n	R^2	Δq (%)	q_m (mg g^{-1})	β (mol^2 J$^2 \times 10^{-9}$)	R^2	Δq (%)
JHC RR2	100				0.85									
	120				0.74									
	140	12.15	0.01	0.927	0.66	5.54	0.25	1.46	0.998	3.12	89.92	5	0.993	29.83
	160				0.59									
	180				0.53									
ZAJHC RR2	100				0.62									
	120				0.45									
	140	100	0.03	0.937	0.35	114.9	5.43	1.63	0.996	112	795.45	4	0.994	114
	160				0.29									
	180				0.25									

is physical in nature [34]. The mean energy of the RR2 adsorption onto JHC and ZAJHC was calculated as 10 and 11.18 kJ mol^{-1}, respectively, which indicates that the adsorption of RR2 onto the JHC and ZAJHC occurred by ion-exchange mechanism.

Figs. 6(a) and (b) show different adsorption isotherms along with the experimental data. In order to compare the validity of isotherms, a normalized deviation, Δq (%), was calculated using the following equation:

$$\Delta q\left(\%\right)=100\times\sqrt{\frac{\sum\left[\left(q_e^{\;exp}-q_e^{\;cal}\right)\middle/q_e^{\;exp}\right]^2}{\left(n-1\right)}} \qquad (6)$$

where superscripts 'exp' and 'cal' are the experimental and calculated values, respectively, and 'n' is the number of

measurements. From the results it was found that Freundlich isotherm shows lowest Δq and so it is most suitable than other isotherms (Table 4).

3.2.8. Effect of temperature

Increase of temperature increased the percent removal. Changes in standard free energy, enthalpy and entropy of adsorption were calculated using the following equations according to van't Hoff equation. JHC and ZAJHC positive values of $\Delta H°$ (60.5 and 12.58 J mol^{-1} K^{-1}) show the endothermic nature of adsorption. The negative values of $\Delta G°$ indicate the spontaneous nature of adsorption for RR2. Table 5 shows positive values of $\Delta S°$ (−9.78 and 64.32 J mol^{-1} K^{-1}) which suggest an increased randomness at the solid/solution interface during the adsorption of dye on JHC and ZAJHC, respectively [35].

Table 5
Thermodynamic parameters for the adsorption of RR2 onto JHC and ZAJHC

	T (K)	K_c	ΔG (kJ mol^{-1})	ΔH (kJ mol^{-1})	ΔS (J mol^{-1} K^{-1})
JHC	308	0.06	7.02		
	313	0.07	6.83	60.5	−9.78
	323	0.07	7.05		
	333	0.07	7.21		
ZAJHC	308	1.54	−1.20		
	313	2.60	−2.49	12.58	64.32
	323	2.29	−2.23		
	333	2.44	−2.47		

4. Conclusions

The effect of pH for maximum removal was found at pH ≥5. The adsorption followed pseudo-second-order kinetics. The equilibrium data followed good fit with Freundlich isotherm. Adsorption of RR2 on JHC was found to non-spontaneous and ZAJHC was found to the spontaneous, respectively. Desorption studies show that the ion-exchange mechanism seems to be the major mode of adsorption for RR2 onto JHC and ZAJHC. The ZAJHC was more suitable for the recovery of adsorbates and there was a possibility of reuse of the adsorbent. ZAJHC can be used as an effective adsorbent for the removal of dyes RR2 from water compared with JHC. ZAJHC to the removal of dyes is expected to be economical.

References

[1] S. Jorfi, R.D.C. Soltani, M. Ahmadi, A. Khataee, M. Safari, Sono-assisted adsorption of a textile dye on milk vetch-derived charcoal supported by silica nano powder, J. Environ. Manage., 187 (2017) 111–121.

[2] M.C. Villalobos, A.A.P. Cid, A.M.H. Gonzalez, Removal of textile dyes and metallic ions using polyelectrolytes and macro electrolytes containing sulfonic acid groups, J. Environ. Manage., 177 (2016) 65–73.

[3] X.Y. Yang, B.A. Duri, Application of branched pore diffusion model in the adsorption of reactive dyes on activated carbon, J. Chem. Eng., 83 (2001) 15–23.

[4] S. Renganathan, J. Kalpana, M. Dharmendira, M. Velan, Equilibrium and kinetic studies on the removal of reactive red 2 dye from an aqueous solution using a positively charged functional group of the *Nymphaea rubra* biosorbent, Clean, 37 (2009) 901–907.

[5] L. Chao, L. Zhaoyang, L. Aimin, L. Wei, J. Zhenmao, C. Jinlong, Z. Quanxing, Adsorption of reactive dyes onto polymeric adsorbents: effect of pore structure and surface chemistry group of adsorbent on adsorptive properties, Sep. Purif. Technol., 44 (2005) 115–120.

[6] O. Duman, S. Tunç, B. Kanci B. Glan, T.G. Polat, Removal of triphenylmethane and reactive azo dyes from aqueous solution by magnetic carbon nanotube-k-carrageenan-Fe$_3$O$_4$ nanocomposite, J. Alloy. Compd., 687 (2016) 370–383.

[7] D. Kavitha, C. Namasivayam, Experimental and kinetic studies on methylene blue adsorption by coir pith carbon, Bioresour. Technol., 98 (2007) 14–21.

[8] E. Ayranci, O. Duman, In-situ UV-visible spectroscopic study on the adsorption of some dyes onto activated carbon cloth, Sep. Sci. Technol., 44 (2009) 3735–3752.

[9] O. Duman, S. Tunç, T.G. Polat, Adsorptive removal of triarylmethane dye (Basic Red 9) from aqueous solution by sepiolite as effective and low-cost adsorbent, Micropor. Mesopor. Mater., 210 (2015) 176–184.

[10] O. Duman, S.Tunç, T.G. Polat, Determination of adsorptive properties of expanded vermiculite for the removal of C.I. Basic Red 9 from aqueous solution: kinetic, isotherm and thermodynamic studies, Appl. Clay Sci., 109–110 (2015) 22–32.

[11] O. Duman, S. Tunc, T.G. Polat, B.K. Bozoglan, Synthesis of magnetic oxidized multiwalled carbon nanotube-carrageenan-Fe$_3$O$_4$ nanocomposite adsorbent and its application in cationic Methylene Blue dye adsorption, Carbohydr. Polym., 147 (2016) 79–88.

[12] R. Subha, C. Namasivayam, Kinetics and isotherms studies on adsorption of phenol using low cost micro porous ZnCl$_2$ activated coir pith carbon, Can. J. Civil Eng., 36 (2009)148–159.

[13] CJP, Centre for Jatropha Promotion and Biodiesel. Available at: http://www.jatrophaworld.org/

[14] K. Ramakrishnan, C. Namasivayam, Zinc chloride-activated jatropha husk carbon for removal of phenol from water by adsorption: equilibrium and kinetic studies, Toxicol. Environ. Chem., 93 (2011) 1111–1122.

[15] A.J. Kumar, C. Namasivayam, Uptake of endocrine disruptor bisphenol-A onto sulphuric acid activated carbon developed from biomass: equilibrium and kinetic studies, Sustain. Environ. Res., 24 (2014) 73–80.

[16] C.S. Ming, Kinetics of the batch adsorption of methylene blue from aqueous solutions onto rice husk: effect of acid-modified process and dye concentration, Desal. Wat. Treat., 37 (2012) 200–214.

[17] J.O. Pezoti, A.L. Cazetta, P.A.F. Isis, Souza, K.C. Bedin, A.C. Martins, T.L. Silva, V. Almeida, Adsorption studies of methylene blue onto ZnCl$_2$-activated carbon produced from buriti shells *Mauritia flexuosa* L, J. Ind. Eng. Chem., 20 (2014) 4401–4407.

[18] F. Caturla, M. Sabio, F.R. Reinoso, Preparation of activated carbon by chemical activation with ZnCl$_2$, Carbon, 29 (1991) 999–1007.

[19] M. Rajesh, V. Veeramani, M.C. Shen, Heteroatom-enriched and renewable banana-stem-derived porous carbon for the electrochemical determination of nitrite in various water samples, Sci. Rep., 4 (2014) 4679.

[20] L. Wang, J. Zhang, R. Zhao, C. Zhang, C. Li, Y. Li, Adsorption of 2,4-dichlorophenol on Mn-modified activated carbon prepared from *Polygonum orientale* Linn., Desalination, 266 (2011) 175–181.

[21] A.C. Lua, T. Yang, Characteristics of activated carbon prepared from pistachio-nut shell by zinc chloride activation under nitrogen and vacuum conditions, J. Colloid Interface Sci., 290 (2005) 505–513.

[22] G. Bharath, R. Madhu, S.M. Chen, V. Veeramani, A. Balamurugan, D. Mangalaraj, C. Viswanathan, N. Ponpandian, Enzymatic electrochemical glucose biosensors by mesoporous 1D hydroxyapatite-on-2D reduced graphene oxide, J. Mater. Chem. B, 3 (2015) 1360–1370.

[23] S.P.J.M. Carrott, M.M.L.R. Carrott, Lignin – from natural adsorbent to activated carbon: a review, Biores. Technol., 98 (2007) 2301–2312.

[24] E. Ayranci, O. Duman, Structural effects on the interactions of benzene and naphthalene sulfonates with activated carbon cloth during adsorption from aqueous solutions, Chem. Eng. J., 156 (2010) 70–76.

[25] O. Dumana, E. Ayranci, Attachment of benzo-crown ethers onto activated carbon cloth to enhance the removal of chromium, cobalt and nickel ions from aqueous solutions by adsorption, J. Hazard. Mater., 176 (2010) 231–238.

[26] E. Ayranci, O. Duman, In-situ UV-visible spectroscopic study on the adsorption of some dyes onto activated carbon cloth, Sep. Sci. Technol., 44 (2009) 3735–3752.

[27] O. Dumana, E. Ayranci, Adsorptive removal of cationic surfactants from aqueous solutions onto high-area activated carbon cloth monitored by in situ UV spectroscopy, J. Hazard. Mater., 174 (2010) 359–367.

[28] A.H. Sulymon, W.M. Abood, Equilibrium and kinetic study of the adsorption of reactive blue, red and yellow dyes onto activated carbon and barley husk, Desal. Wat. Treat., 52 (2014) 5485–5493.

[29] I. Langmuir, The adsorption of gases on plane surface of glass. Mica and platinum, J. Am. Chem. Soc., 40 (1918) 1361.

[30] H. Freundlich, Uber die adsorption in Losungen, Z. Phys. Chem., 57 (1906) 387–470.

[31] O. Duman, E. Ayranci, Structural and ionization effects on the adsorption behaviors of some anilinic compounds from aqueous solution onto high-area carbon-cloth, J. Hazard. Mater., 120 (2005) 173–181.

[32] O. Duman, E. Ayranci, Adsorption characteristics of benzaldehyde, sulphanilic acid, and p-phenol sulfonate from water, acid, or base solutions onto activated carbon cloth, Sep. Sci. Technol., 41 (2006) 3673–3692.

[33] E. Ayranci, O. Duman, Removal of anionic surfactants from aqueous solutions by adsorption onto high area activated carbon cloth studied by in situ UV spectroscopy, J. Hazard. Mater., 148 (2007) 75–82.

[34] K. Kannan, M.M. Sundaram, Kinetics and mechanism of removal of methylene blue by adsorption on various carbons – a comparative study, Dyes Pigm., 51 (2001) 25–40.

[35] C. Namasivayam, S. Sumithra, Removal of direct red 12B and methylene blue from water by adsorption onto Fe (III)/Cr (III) hydroxide, an industrial solid waste, J. Environ. Manage., 74 (2005) 207–215.